JOURNAL OF GEOPHYSICAL RESEARCH, VOL. 104, NO. C7, PAGES 15,669–15,677, JULY 15, 1999

An energy-conserving thermodynamic model of sea ice

C.M. Bitz[1]
Department of Earth and Ocean Sciences, University of Victoria, British Columbia, Canada

William H. Lipscomb[2]
Department of Atmospheric Sciences, University of Washington, Seattle

Abstract. We introduce an energy-conserving sea ice model for climate study that accounts for the effect of internal brine-pocket melting on surface ablation. Sea ice models that parameterize latent heat storage in brine pockets often fail to reduce the energy required for surface ablation in proportion to the internal melting that has already occurred. These models do not conserve energy during the summer melt season. Compared with our energy-conserving model, a nonconserving model underestimates top-surface ablation of multiyear ice by 12–22% and overestimates the equilibrium ice thickness by 50–124 cm. In addition, a nonconserving model is less sensitive to perturbative forcing than our energy-conserving model is: The equilibrium thickness changes 22–44% less owing to surface albedo perturbations and 13–31% less owing to downward longwave radiation perturbations. The smaller differences are associated with a model that has a time-independent, vertically varying salinity profile, and the larger differences are associated with a model that assumes the ice is isosaline with a salinity of 3.2‰. Simulations with a vertically varying salinity profile have low salinity at the top surface compared to isosaline cases, which leads to reduced heat conduction, less internal brine-pocket melting, and more surface ablation.

1. Introduction

The important role of the high latitudes in global climate has motivated efforts to improve sea ice models by using more realistic thermodynamics. "Realism" should be added to these models in a way that conserves energy (and, of course, water). Currently, most climate models use variations of the zero-layer or three-layer ice model from *Semtner* [1976]. While these models do a reasonably good job of conserving energy, they lack generality and validity in certain respects [*Semtner*, 1984].

A physically realistic model of sea ice should accurately represent the heat capacity (the energy needed to raise the temperature of a unit mass of ice by 1°C) and energy of melting (the energy required to melt a unit volume of ice), which differ from the values for pure ice, especially near 0°C. The difference is due mainly to brine pockets, which change size in order to remain in thermal equilibrium with the ice [*Schwerdtfeger*, 1963]. As the ice cools, water in the brine pockets must freeze so that the brine-pocket salinity increases to the value appropriate for the lower temperature. Similarly, as the ice warms, the brine pockets must become less saline, which is achieved by melting ice along the walls of the brine pockets. Thus the heat capacity of sea ice includes not only the energy required to raise the temperature of pure ice but the energy needed to raise the temperature of brine and to melt ice along the walls of brine pockets. The energy required to melt the remaining ice is less than it would be for an equal volume of pure ice because of the internal melting that has already occurred.

As the ice nears 0°C, brine pockets can occupy a significant fraction of the total volume. In multiyear Arctic ice the porosity (i.e., the volume of brine and air per unit volume of sea ice) often reaches 20–30% in the upper 30 cm [*Eicken et al.*, 1995] and may be as large as 40–50% beneath old melt ponds [*Maykut et al.*, 1992]. The energy of the melting of sea ice should be reduced in proportion to the porosity. However, many sea ice models with a salinity-dependent expression for the heat capacity (e.g., *Maykut and Untersteiner* [1971], hereinafter referred to as MU71, and *Ebert and Curry* [1993]) do not make an appropriate correction to the latent heat of melting at the upper surface to account for internal brine-pocket melting. These models apply more energy than is necessary to melt ice at the upper surface and as a result do not conserve energy. This is an error that we aim to correct in this paper.

[1]Now at Quaternary Research Center, University of Washington, Seattle.

[2]Now at Group T-3 Los Alamos National Laboratory, Los Alamos, New Mexico.

Paper number 1999JC900100.
0148-0227/99/1999JC900100$09.00

First we derive expressions for the heat capacity and the energy of melting of sea ice as functions of temperature and salinity in section 2. Then in section 3 we show how to use these expressions in a sea ice model in a way that conserves energy. In section 4 we compare our new energy-conserving model to a version of our model that does not make the appropriate correction when melting. We explore the differences between these two methods with a series of sensitivity experiments. We also compare our new energy-conserving model to the *Semtner* [1976] zero- and three-layer models. Finally we discuss these results and give conclusions in sections 5 and 6.

2. Theory

Exploration of the thermal properties of sea ice by *Malmgren* [1927] led *Untersteiner* [1961] to propose a relatively simple approximation for the heat capacity of sea ice:

$$c(T,S) = c_o + \frac{\gamma S}{T^2}, \tag{1}$$

where $c_o = 2110$ J kg^{-1} deg^{-1} is the heat capacity of fresh ice, S is the salinity in parts per thousand (‰), and T is the temperature in Celsius. Untersteiner let $\gamma = 4100$ cal deg g^{-1} (17.2 kJ deg kg^{-1}) on the basis of values for heat capacity tabulated by Malmgren. Later, *Ono* [1967] pointed out that (1) can be derived from first principles such that

$$\gamma = L_o \mu \tag{2}$$

after ignoring terms that are negligibly small. Equation (2) defines γ based on L_o, the latent heat of fusion of fresh ice, at 0°C and μ, the empirical constant from the relationship between the melting temperature and salinity of sea ice:

$$T_m = -\mu S. \tag{3}$$

With $L_o = 334$ kJ kg^{-1} and $\mu = 0.054°$ as determined by *Assur* [1958], we find $\gamma = 18.0$ kJ deg kg^{-1}, just 5% higher than Untersteiner's 1961 value.

Equation (1) can be multiplied by the sea ice density ρ and integrated to give the amount of energy Q required to raise the temperature of a unit volume of sea ice from T to T':

$$Q(S,T,T') = \rho c_o (T' - T) - \rho L_o \mu S \left(\frac{1}{T'} - \frac{1}{T}\right). \tag{4}$$

Suppose we let $T' = T_m$. At this temperature the unit volume of sea ice should consist entirely of brine; that is, the melting is complete. We find that q, the amount of energy needed to melt a unit volume of sea ice of salinity S at temperature T, resulting in meltwater at T_m, is equal to

$$q(S,T) = \rho c_o (T_m - T) + \rho L_o \left(1 + \frac{\mu S}{T}\right). \tag{5}$$

We refer to q as the *energy of melting* of sea ice; its units are J m^{-3}. For $S = 0$ the energy of melting is what we would expect for pure ice: a heat capacity term equal to the energy required to raise the temperature to 0°C and a latent heat term equal to the energy required to melt the ice. Although q is undefined at 0°C, it is well behaved up to T_m, at which point $q = 0$ and the ice is completely melted. Hence, over the range of relevant temperatures, there is not a singularity in (1) or (5), as some authors have assumed, and there is no need to stipulate a maximum value (e.g., −0.1°C) above which the temperature of sea ice cannot rise. The density of sea ice that appears in (4) and (5) represents a local average over regions of pure ice and brine pockets and is assumed to be constant ($\rho = 917$ kg m^{-3}). The factor $\rho(1 + \mu S/T)$ in the second term of (5) is equivalent to the mass of unmelted ice per unit volume of sea ice (i.e., the mass of the sea ice minus the mass of the brine per unit volume).

Schwerdtfeger [1963] also derived an expression for the heat capacity of sea ice. However, he ignored the temperature dependence of the energy of melting of pure ice, and as a result, he obtained the extra term $(c_w - c_o)\mu S/T$ in his expression for the heat capacity (his equation (1.3.7)), where c_w is the heat capacity of pure liquid water. Had he used the more accurate expression for the energy of melting of pure ice, the extra term would have canceled and he would have derived the simpler result (equation (1)).

We have argued that if sea ice reaches the melting temperature, no additional energy is needed to melt the ice. Thus ablation and accretion of sea ice depend on the energy of melting,

$$F(T) = -q(S,T)\frac{dh}{dt}, \tag{6}$$

where F is the net flux toward the top or bottom surface, h is the ice thickness, and t is time. Herein lies the problem with past sea ice models that use a salinity-dependent heat capacity (i.e., equation (1)). To our knowledge, all of these models (except that of *Björk* [1992]) assume that q in (6) is equal to ρL_o when computing ablation rates at the top surface [e.g., MU71; *Gabison*, 1987; *Ebert and Curry*, 1993; *Bitz et al.*, 1996; *Flato and Brown*, 1996]. Near the melting temperature, however, q is significantly smaller than ρL_o (Figure 1). Use of the proper expression for q is especially important at the top surface when the temperature approaches T_m, because (5) implies that q approaches zero as T approaches T_m for any nonzero salinity.

Some modelers [e.g., MU71; *Ebert and Curry*, 1993] assume that q at the bottom of the slab is about 10% less than ρL_o. Sea ice is in contact with the ocean, which is typically very near its freezing temperature. According to (5), $q = 0.92 L_o$ when $T = -2$°C and $S = 3.2$‰, where S is chosen to be representative of the salinity near the base of multiyear ice [*Weeks and*

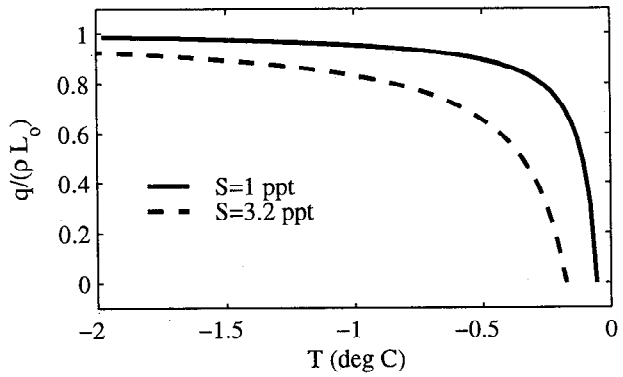

Figure 1. Energy of melting relative to the latent heat of fusion of pure ice as a function of temperature for $S = 3.2‰$ and $S = 1‰$.

Ackley, 1986]. Hence the assumption that $q = 0.9L_o$ at the bottom of the sea ice does not lead to large errors in bottom-surface accretion and ablation rates.

A limitation of our model is the assumption of constant density ρ. During the melt season a layer of deteriorated ice 5-10 cm thick is often observed at the top surface, with a density of 500 kg m^{-3} or less. Beneath this deteriorated ice, multiyear ice contains air-filled pores that can reduce its density to $700 - 800$ kg m^{-3} in the upper 30–50 cm [*Eicken et al.*, 1995]. By fixing the density our model implicitly assumes that all drained brine pockets are filled not with air but with meltwater. Thus the model will underestimate the rate of cooling of the upper ice layers in the fall and the rate of warming of these layers in the spring. Our model does, however, keep an energy-conserving account of the total mass of unmelted ice, which we believe is of greater importance. Future modelers may wish to treat upper surface melt processes in greater detail and incorporate a depth-dependent density profile.

The consequences of neglecting to use the complete expression for the energy of melting depend on the formulation of the model and the context in which it is used. We will explore these issues further in the following sections. Before proceeding, however, we want to emphasize that to conserve energy in a sea ice model that has an explicit brine-pocket parameterization, it is imperative to use the proper expression for the energy of melting.

3. Energy-Conserving Model

3.1. Additional Equations

Vertical heat conduction and storage in the sea ice are governed by the heat equation, modified to include internal absorption of solar radiation:

$$\rho c \frac{\partial T}{\partial t} = \frac{\partial}{\partial z} k \frac{\partial T}{\partial z} + \kappa I_0 e^{-\kappa z}, \tag{7}$$

where k is the conductivity, I_0 is the solar radiation that penetrates the upper surface, and $\kappa = 1.5$ m^{-1} [*Untersteiner*, 1961] is the extinction coefficient from Beer's law. Because the heat capacity of sea ice is a function of temperature, from (4) and (7) we have

$$\int_T^{T'} \rho c dT = \rho c_o (T' - T) \left(1 + \frac{L_o \mu S}{c_o T' T}\right)$$

$$= \int_t^{t'} \left(\frac{\partial}{\partial z} k \frac{\partial T}{\partial z} + \kappa I_0 e^{-\kappa z}\right) dt. \tag{8}$$

where T and T' are the initial and final temperatures, respectively. Equation (8) is an expression of the first law of thermodynamics: The change in internal energy is equal to the heat entering a layer dz. If the integral on the left in (8) is evaluated holding the heat capacity fixed at $c(T, S)$ (as previous thermodynamic models have often done), then energy is not conserved when $S > 0$.

To model heat conduction and storage, we use a model with a fixed number of layers, N, in the ice and one layer of snow (see Figure 2). The energy-conserving model solves the finite difference form of the nonlinear (8) using an implicit backwards-Euler, space-centered scheme with a Newton-Raphson method for coupled equations. Documentation for the numerical solution to (8) is given by *Lipscomb* [1998].

Brine pockets also influence the thermal conductivity of ice, which is

$$k(S, T) = k_o + \frac{\beta S}{T}, \tag{9}$$

where $k_o = 2.034$ W m^{-1} deg^{-1} is the conductivity of fresh ice and β is 0.117 W m^{-1} ‰$^{-1}$, following *Untersteiner* [1964].

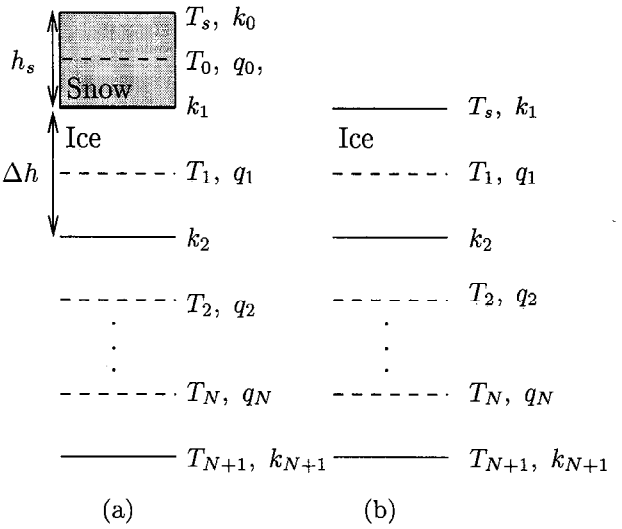

Figure 2. Vertical grid of the sea ice (a) when snow is present and (b) when the ice is snow-free. The value Δh is the thickness of each ice layer, and h_s is the thickness of the snow layer. The surface temperature in either case is T_o.

Boundary conditions for (8) follow from the top-surface flux balance and from the temperature of the ocean layer as described below. The top-surface flux balance is

$$F_{\rm net}(T_o) = F_r(1-\alpha) - I_0 + F_L - \sigma T_o^4 + F_s + F_e + k\frac{\partial T}{\partial z}, \quad (10)$$

where $F_r(1-\alpha)$ is the net downward solar radiation at the top surface, α is the surface albedo, I_o is the solar radiation that penetrates the top surface, F_L is the downward longwave radiation, σT_o^4 is the outgoing longwave radiation (for T_o in kelvin), F_s and F_e are the downward sensible and latent heat fluxes, respectively, and $k\partial T/\partial z$ is the conductive flux from the sea ice/snow interior toward the top surface. If $F_{\rm net}(T_m) \geq 0$, then the upper surface is fixed at the melting temperature (see section 3.3 for a discussion of the upper surface melting temperature) and ablation occurs according to (6). If $F_{\rm net}(T_m) < 0$, then the upper surface is not melting and T_o is found by solving $F_{\rm net}(T_o) = 0$.

The bottom temperature of the sea ice is fixed at T_f, the freezing temperature of seawater, which we assume is -1.95°C, following MU71. The bottom-surface flux balance is

$$F_w - k\frac{\partial T}{\partial z} = -q(S,T)\frac{dh}{dt}, \quad (11)$$

where F_w is the heat flux from the ocean (see section 3.4) and $k\partial T/\partial z$ is the conductive flux from the bottom surface toward the interior.

The snow is assumed to be fresh, so that the heat capacity and latent heat of snow are c_o and L_o, respectively. The density of snow is $\rho_s = 330$ kg m^{-3}, and the energy of melting for snow is $q_s(T) = -\rho_s c_o T + \rho_s L_o$. The conductivity of snow is assumed to be $k_s = 0.31$ W m^{-1} K^{-1}.

3.2. Salinity Profile

It has been suggested that the salinity profile of multiyear ice is nearly steady over time [*Maykut et al.*, 1992]. Thus thermodynamic sea ice models often assume a time-independent salinity profile based on observations from the work of *Schwarzacher* [1959], which has low salinity near the upper surface (e.g., MU71). Another strategy has been to assume that the ice is isosaline [e.g., *Ebert and Curry*, 1993], where the mean salinity is determined empirically from the thickness based on estimates by *Cox and Weeks* [1974], and sea ice thicker than 60 cm has a salinity of 3.2‰.

For sake of comparison to previous studies of multiyear sea ice with thermodynamic models, we explore the sensitivity of our model to two idealized salinity profiles, both of which are assumed to be fixed in time. The first is isosaline, with $S_l = 3.2$‰ in each layer l, and the second has a vertically varying salinity dependence:

$$S_l = 1.6 - 1.6\cos\left[\pi\left(\frac{l-0.5}{N}\right)^{\frac{n}{m+(l-0.5)/N}}\right], \quad (12)$$

after MU71, where $n = 0.407$ and $m = 0.573$ are determined from a least squares fit to the profile by *Schwarzacher* [1959]. This profile varies from 0‰ at the top to 3.2‰ at the bottom surface.

3.3. Top-Surface Temperature Boundary Condition

Meltwater draining through sea ice above freeboard during summer flushes away brine near the upper surface [e.g., *Weeks and Ackley*, 1986]. Hence the salinity of multiyear sea ice tends to decrease toward the upper surface, arriving at a nearly fresh surface layer several centimeters thick. For this reason we allow the upper surface ice temperature, T_o, to reach 0°C during the melt season when we use the vertically varying salinity profile from (12). When we use an isosaline profile, the melting temperature of the upper surface should lie between -0.17°C (from equation (3)) and 0°C depending on the salinity at the boundary. We assume $T_o = -0.10$°C for melting ice, following *Ebert and Curry* [1993]. Because the snow is fresh, the upper snow surface is allowed to reach 0°C independent of sea ice salinity.

During the melt season the boundary condition for the heat equation is higher than the range of temperatures at which q for saline ice is defined. This is not a problem, however, because the underlying seawater is colder than the upper ice surface, creating a temperature gradient in the ice that prevents the internal layer temperatures from reaching T_m, let alone -0.1° or 0°C. However, if an internal temperature did reach T_m, the layer would be completely melted and the total ice thickness could be reduced accordingly.

3.4. Forcing and Parameter Specification

We use the model forcing from the standard case in MU71, which is based on the work of *Fletcher* [1965]. The heat flux from the ocean, F_w, is assumed to be a constant 2 W m^{-2}. The fraction i_o of solar radiation that penetrates the upper ice surface is assumed to be $0.3[10/(h_s + 10)]$, after *Bettge et al.* [1996], for h_s in centimeters (except in section 4.4, where i_o is redefined to be consistent with that in the *Semtner* [1976] three-layer model). For the albedo we assume $\alpha_s = 0.80$ for dry snow, $\alpha_s = 0.75$ for melting snow, and $\alpha_i = 0.63$ for bare ice, unless otherwise noted. The bare ice albedo is the only parameter that is tuned in order to reach a reasonable equilibrium thickness of approximately 300 cm. The model is integrated with a 4-hour time step and $N = 10$, unless otherwise noted.

4. Results

Next we examine the equilibrium ice thickness and the phase and amplitude of the annual thickness cycle for various model configurations. We explicitly compute the heat entering the ice-snow system from the

atmosphere and ocean and compare it to the storage of energy in the sea ice. We test the sensitivity of the model to decreasing the bare ice albedo by 0.01 and to increasing the net longwave radiation by 1 W m^{-2}. Finally we compare our model to the *Semtner* [1976] zero- and three-layer models.

4.1. Sensitivity of sea Ice Thickness to Internal Brine-Pocket Melting

Beginning with the vertically varying salinity profile, we compare results for (1) an energy-conserving model which accounts for internal brine-pocket melting using the proper expression for q and (2) an energy nonconserving model where internal melting is neglected by letting $q = \rho L_o$ at the top surface and $q = 0.92\rho L_o$ at the bottom surface in equation (6) (also $q_s = \rho_s L_o$ as is often the case in other models). Figure 3a shows the first annual cycle after initializing both models with the same ice thickness and temperature profile. Although both models are forced in the same way, the amplitude of the annual cycle of ice thickness (defined as the maximum from the first winter minus the minimum from the first melt season) for the nonconserving model is 12% less than that for the conserving model. The difference arises mainly from the increased melt rate for the conserving model. Nonetheless, the length and phase of the melt seasons are nearly the same.

These different melt rates yield substantially different equilibrium thicknesses. The annual mean thickness for the first 50 years of the integration is shown in Figure 3b. The equilibrium thickness for the nonconserving model is 331 cm, which is 50 cm greater than that for the conserving model. (Equilibrium thickness is defined as the annual mean thickness in the last year of a 100-year integration. By the end of 100 years the annual mean thickness changes by much less than 1 cm yr^{-1}.) The results from this pair of experiments and those following are summarized in Table 1.

This comparison shows how the correct treatment of internal melting would affect the ice thickness in a model like that of MU71, which used a similar salinity profile. The integrations in Figure 3 have only 10 layers (or layers about 30 cm thick), so our temperature resolution in Figure 3 is coarser than that in MU71, which specified layers 10 cm thick. However, the model results are very similar with 30 layers (or layers 10 cm thick).

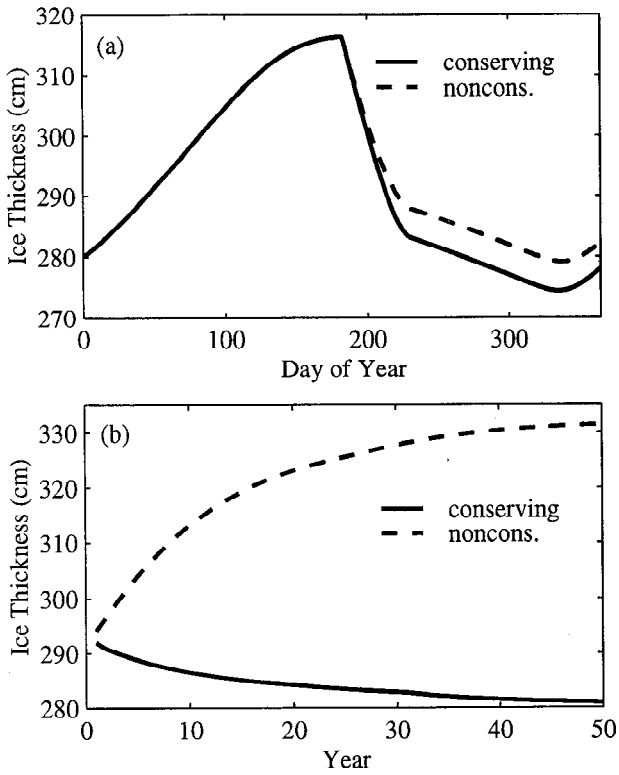

Figure 3. Comparison of ice thickness for energy-conserving (solid curves) and nonconserving (dashed curves) models for vertically varying salinity profile: (a) first annual cycle and (b) annual mean for first 50 years.

Although our nonconserving model closely approximates that of MU71, the annual cycle and equilibrium thickness differ from the standard case in MU71 because we allow a higher fraction of solar radiation to penetrate the top ice surface (following *Grenfell and Maykut* [1977], we set $i_o = 0.30$ for bare ice, compared with $i_o = 0.17$ in MU71), and our bare ice albedo is 1% lower. See MU71 and the work of *Semtner* [1984] for more information on how the ice thickness depends on i_o.

Next we perform the same experiments for isosaline ice with $S_l = 3.2‰$. Figure 4a shows the first annual cycle for both conserving and nonconserving models with $\alpha_i = 0.63$ as in Figure 3a. Ablation at the top surface is greatly reduced, and the equilibrium thickness is much

Table 1. Summary of Results From Experiments for Conserving and Nonconserving Methods

Experiment Description		h_{eq}, cm		Ampl. of h, cm		Max $\lvert F_{err}\rvert$, W m^{-2}	
Salinity	α_i	Cons.	Noncons.	Cons.	Noncons.	Cons.	Noncons.
Vertically varying	0.63	281	331	42	37	$\sim 10^{-4}$	4.0
Isosaline	0.63	400	502	34	27	$\sim 10^{-5}$	5.9
Isosaline	0.60	259	383	41	32	$\sim 10^{-5}$	7.4

Result include equilibrium thickness h_{eq}, amplitude (ampl.) of first annual cycle for ice thickness h, and the maximum amplitude for F_{err} of equation (13). cons., conserving; noncons., nonconserving.

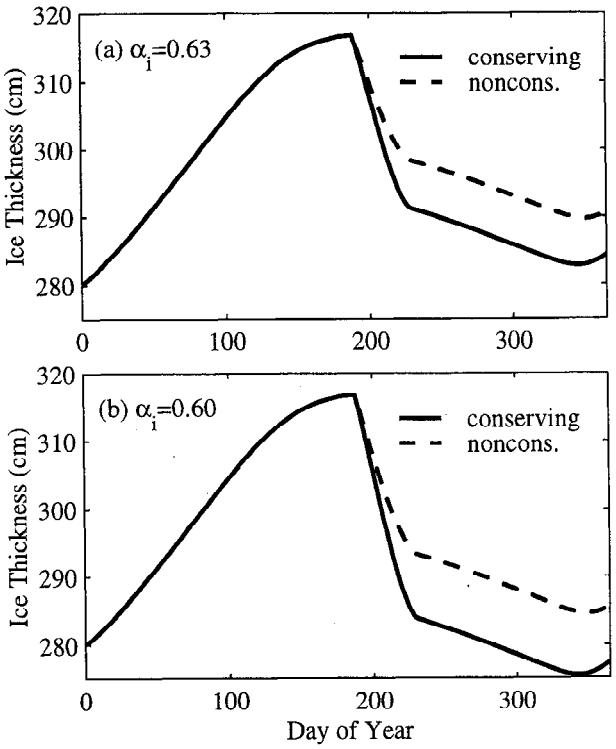

Figure 4. Comparison of ice thickness for energy-conserving (solid curves) and nonconserving (dashed curves) models for the isosaline profile. The bare ice albedo is varied from (a) $\alpha_i = 0.63$ to (b) $\alpha_i = 0.60$.

greater (see Table 1) for this pair of experiments compared with those above with vertically varying salinity. For the purpose of comparing energy-conserving and nonconserving models for ice approximately 300 cm thick, we reduce the bare ice albedo to $\alpha_i = 0.60$ and repeat the experiments (see Figure 4b). The amplitude of the annual cycle is now 22% lower, and the equilibrium thickness is 124 cm greater for the nonconserving model as compared with the conserving model. This larger error can be explained as follows: With higher salinity near the top surface the upper ice layers have a lower temperature, and more heat is conducted from the top surface to the ice interior. This heat causes additional internal melting, which in the case of the nonconserving model is neglected when computing subsequent ablation at the top surface.

Table 1 shows that the ice thickness is quite sensitive to the salinity profile. For the energy-conserving model with $\alpha_i = 0.63$ the equilibrium thickness is 400 cm with the isosaline profile, compared with just 281 cm with the vertically varying profile. Thus models that assume an isosaline profile of 3.2‰ will tend to overestimate the thickness of multiyear Arctic ice, for which the vertically varying profile is more appropriate.

This result shows the importance of modeling the salinity profile realistically. In a climate model that includes many kinds of ice with different salinity profiles (e.g., firstyear and multiyear and Arctic and Antarctic), it would be desirable to predict the evolution of the salinity profile over time. The model would need to parameterize desalination processes such as brine expulsion, brine drainage, and flushing [*Untersteiner*, 1968]. We have recently developed such a model, which successfully simulates the transition from the typical C-shaped profile of first-year ice to the profile of multiyear ice. This prognostic salinity model will be used in forthcoming climate simulations.

4.2. Energy Loss Associated with Neglecting Internal Brine-Pocket Melting

To diagnose the magnitude of the energy lost by the nonconserving model, the flux of heat to the ice and snow should be equal to the change per unit time in the vertically integrated internal energy. For backwards-Euler time stepping, we define an error for the energy conservation in flux form:

$$F_{\rm err}^{j+1} = F_{\rm net}^{j+1} - F_{rb}^{j+1} + F_w^{j+1} - (h_s^{j+1} q_s^{j+1} - h_s^j q_s^j)/\Delta t - \left(\Delta h^{j+1} \sum_{l=1}^{N} q_l^{j+1} - \Delta h^j \sum_{l=1}^{N} q_l^j \right) / \Delta t, \quad (13)$$

where j is the time index and F_{rb}^{j+1} is the solar radiation that passes through the bottom of the sea ice. (The heat associated with falling snow is not included in (13).) Figure 5 shows the annual cycle of $F_{\rm err}$ for the energy nonconserving model with both vertically varying salinity (as in Figure 3) and isosaline ice (with $\alpha_i = 0.60$ for bare ice, as in Figure 4b). $F_{\rm err}$ is negligible until snow begins to melt, which leads to a small positive error from neglecting $-\rho_s c_o T$ in q_s when computing the snow melt rate. Once the sea ice begins to melt, $F_{\rm err}$ becomes strongly negative because the terms $\rho c_o (T_m - T) + \rho L_o \mu S/T$ in (5) are neglected when computing the melt rate. Most of the error comes from the second term, which accounts for internal brine-pocket

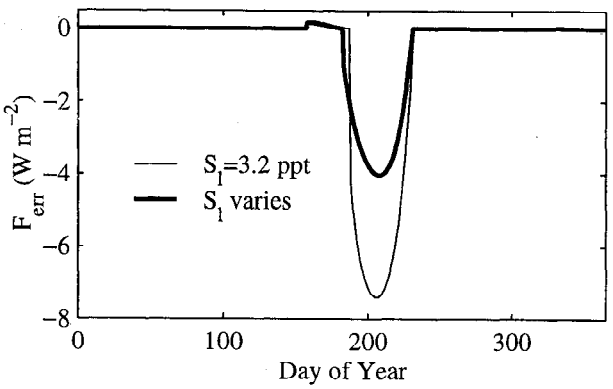

Figure 5. Annual cycle of $F_{\rm err}$ for integrations with vertically varying salinity profile and isosaline profile with $\alpha_i = 0.60$ for bare ice. (Multiply by 86.4 to convert $F_{\rm err}$ into energy in kilojoules lost per day.)

Table 2. Equilibrium Thickness Change Due to Perturbative Forcing for Conserving and Nonconserving Models and for Vertically Varying and Isosaline Profiles

Salinity	Decrease α_i by 0.01		Increase F_L by 1 W m^{-2}	
	Cons.	Noncons.	Cons.	Noncons.
Vertically varying	27	21	-48	-41
Isosaline	39	22	-77	-53

Equilibrium thickness is in centimeters. cons., conserving; noncons., nonconserving.

melting. The largest error occurs near the middle of the melt season when $F_{\rm err}$ is -4.0 W m^{-2} for the vertically varying salinity profile and -7.4 W m^{-2} for isosaline ice. Averaged over the period when the ice is melting at the top surface, $F_{\rm err} = -2.9$ W m^{-2} for the vertically varying salinity profile and -5.6 W m^{-2} for isosaline ice. For the energy-conserving model, $|F_{\rm err}| < 10^{-4}$ W m^{-2} all year.

Internal brine-pocket melting (the primary source of $F_{\rm err}$) results from penetrating solar radiation, I_o, that is absorbed in the ice interior and, to a lesser extent, from convergence of heat by conduction. I_o depends on the net solar radiation at the surface and the snow depth. During the melt season, I_o averages 8 W m^{-2}, of which about 3 W m^{-2} is absorbed in the portion of the ice that eventually melts during that melt season. Hence $F_{\rm err}$ for the vertically varying salinity case is due almost entirely to I_o. For the isosaline case, convergence of heat by conduction in the upper ice layers contributes an additional 3 W m^{-2}, approximately doubling $F_{\rm err}$.

4.3. Sensitivity of the Model to Perturbations in Surface Albedo and Downward Longwave Radiation

We test the sensitivity of the model to perturbative forcing by (1) decreasing the bare ice albedo by 0.01 and (2) increasing the downward longwave radiation at the surface by 1 W m^{-2} all year (Table 2). To compare the sensitivity of energy-conserving and nonconserving models for both salinity profiles, it is important to perturb the various models from approximately the same basic state. This is accomplished by tuning α_i so that the equilibrium thickness is between 281 and 297 cm and the amplitude of the annual cycle is between 37 and 42 cm.

Compared to the energy-conserving model, the equilibrium thickness of the nonconserving model is less sensitive by 22–44% to α_i perturbations and by 13–31% to F_L perturbations. The larger differences occur when the model has an isosaline profile. Directly varying the net solar radiation by perturbing α_i leads to greater disparity in the response of the two models, because changes in the solar radiation affect internal melting directly, while changes in the longwave radiation affect internal melting only indirectly by altering the surface energy balance.

4.4. Comparison of Energy-Conserving Model with the Zero- and Three-Layer Models

Next we compare our model to the zero- and three-layer models from *Semtner* [1976] using the same forcing as that described in section 3.4. We specify a vertically varying salinity profile for both energy-conserving and nonconserving models. We modify the fraction of solar radiation that is allowed to penetrate the surface, because Semtner's three-layer model allows solar radiation to penetrate the surface only when the ice is free of snow. Hence, for Semtner's model and our energy-conserving and nonconserving models, we use $i_o = 0.30$ when the surface is snow-free and $i_o = 0$ otherwise. The zero-layer model does not allow solar radiation to penetrate the upper surface at all. To compensate, we modify the bare ice albedo and the ice conductivity for the zero-layer integrations, as suggested by Semtner. We use the same heat of fusion at top and bottom surfaces in the zero- and three-layer models to avoid fictitious energy sinks. Semtner used a 10% smaller heat of fusion at the bottom of the ice to compare his model to MU71.

Figure 6a shows the results from all four integrations. The amplitude of the first annual cycle in the *Semtner* [1976] three-layer model is 50 cm, about 5% greater than that for our conserving model (48 cm) and 15% greater than that for the nonconserving model (42 cm). The equilibrium thickness (Figure 6b) of Semtner's three-layer model is 235 cm, 10% less than that for the conserving model (162 cm) and 26% less than that for the nonconserving model (316 cm). While Semtner found very close agreement between the equilibrium thickness of the three-layer model and the MU71 model, we find that the three-layer model yields much thinner ice than the nonconserving model does (a close approximation to MU71). This occurs because unlike Semtner, we use the same latent heat of fusion at the top and bottom of the ice in the three-layer model.

Consistent with the results of *Semtner* [1976], the zero-layer model overestimates the amplitude of the annual cycle of the sea ice thickness by about 50% com-

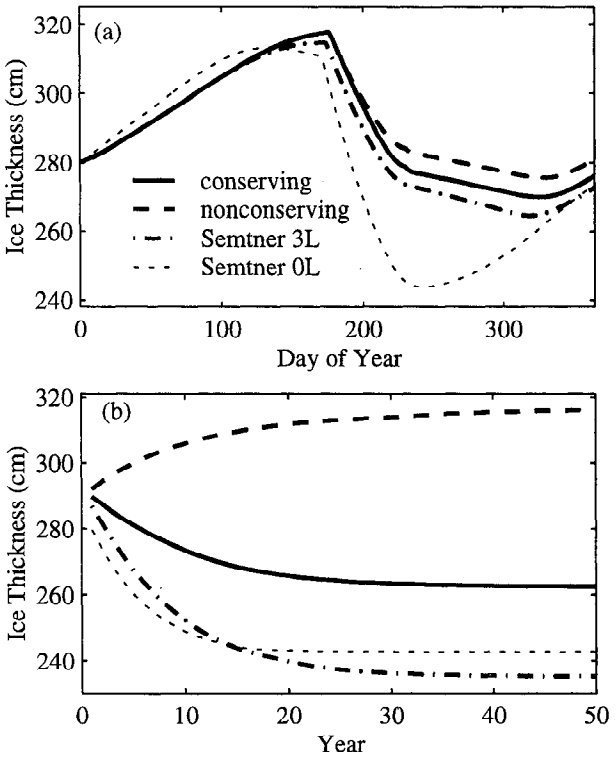

Figure 6. Comparison of ice thickness for energy-conserving (solid curves) and nonconserving (dashed curves) models (with vertically varying salinity profile) and the *Semtner* [1976] three-layer (dash-dotted curves) and zero-layer (dashed curves) models: (a) first annual cycle and (b) annual mean for first 50 years.

pared with the more complex models. The equilibrium thickness predicted by the zero-layer model (243 cm) is less than that of the energy-conserving model.

The energy conservation error $F_{\rm err}$ was computed (with modifications to (13) to include energy stored in the brine-pocket reservoir) for the zero- and three-layer models (not shown). The errors are usually small ($F_{\rm err} \lesssim 0.25$ W m^{-2}) and can be eliminated altogether with minor changes to the code.

5. Discussion

The energy-conserving model includes the important effect of internal brine-pocket melting on the energy of melting at the top surface. Neglecting this effect decreases top-surface ablation by 12–22% and increases the equilibrium thickness by 50–124 cm for multiyear ice that is approximately 300 cm thick.

We examined the effects of energy nonconservation on multiyear ice in the central Arctic. Our results are conservative compared to what might be expected in regions of seasonal ice where the absorbed solar radiation is greater. Increasing the solar radiation would increase the energy absorbed internally by ice that melts during the same season. Thus the difference in surface ablation between the conserving and nonconserving models would be greater.

Compared to the energy-conserving model, the equilibrium thickness of the nonconserving model is 22–44% less sensitive to perturbations in the surface albedo and 13–31% less sensitive to perturbations in the downward longwave radiation. In light of these substantial differences we believe some of the previous results using nonconserving models should be reexamined. In particular, studies of sea ice sensitivity to changes in the net solar radiation (e.g., through changes in surface albedo or cloud parameterizations) may be in error. Previous models must also have been tuned to achieve a reasonable equilibrium ice thickness while failing to conserve energy.

The salinity profile affects top-surface ablation considerably. Near the surface, high salinity leads to steep temperature gradients and substantial heat conduction from the surface to the ice interior. As a result, there is less melting at the top surface and more melting internally. If this internal melting is subsequently neglected when computing top-surface melting, the model predicts much less ablation and a much greater equilibrium ice thickness.

The isosaline profile is representative of first-year sea ice that is observed at the end of the winter. Multiyear sea ice that is approximately isosaline has been observed in Antarctica [*Eicken*, 1992], where flushing is nearly absent, and in depressions (ice with below-average freeboard height) in the Arctic during winter [*Cox and Weeks*, 1974]. However, most observations of the salinity of multiyear ice resemble the *Schwarzacher* [1959] profile of (12) [e.g., *Cox and Weeks*, 1974; *Tucker et al.*, 1987; *Eicken et al.*, 1995]. Given the strong dependence of summer ablation on salinity, improved understanding of desalination processes could be an important step toward realism in sea ice modeling.

Semtner [1976] developed the three-layer model to simplify the model of MU71. In Semtner's model, solar energy that penetrates beneath the ice surface during snow-free periods is stored in a fictitious heat reservoir. This energy does not contribute to surface melting in the summer but instead delays cooling in the fall. To obtain better agreement with MU71, Semtner specified a latent heat of fusion at the bottom of the ice that is 10% lower than that at the top. Semtner noted that using inequivalent latent heats of fusion implies an unphysical heat sink in the ice. In our implementation of Semtner's three-layer model, we avoid such sinks, and the results agree much more closely with our energy-conserving model than with the nonconserving model.

6. Conclusions

Compared to the energy-conserving model, the equilibrium ice thickness is (1) 50 cm greater for the nonconserving model with a vertically varying salinity profile, because internal melting, due primarily to absorbed so-

lar radiation, is neglected for ice that melts at the top surface later in the season, and (2) 124 cm greater for the nonconserving model with an isosaline profile, because the internal melting that is neglected includes not only absorbed solar radiation but also substantial heat conduction from the top surface to the ice interior.

We acknowledge that although these differences are substantial, similar changes could be obtained by adjusting the bare ice albedo by a few percent or by adding a melt-pond parameterization. However, neglecting the effect of brine-pocket melting on upper surface ablation is particularly important because it involves energy conservation. Failure to conserve energy by a few watts per square meter in a coupled atmosphere-ice-ocean model can bias long-term results.

Our new model conserves energy to high precision and is thus suitable for applications where energy conservation is desirable (e.g., coupled climate modeling). The energy-conserving model has been successfully coupled to an ocean general circulation model by one of us (C. M. Bitz). The numerical solution for the evolution of the sea ice thermodynamics as described in sections 2 and 3 comprises approximately one-third of the total time required to integrate the coupled global ice-ocean system when the time step for the ice is one-fifth that of the ocean. Hence our model is efficient for long-term global simulations.

Acknowledgments. We thank B. Briegleb, M. Holland, G. Maykut, W. Tucker III, N. Untersteiner, and S. Warren for helpful suggestions. We thank A. Semtner Jr. for providing the code for the zero- and three-layer models. This work was completed while CMB was supported by the Canadian Institute for Climate Studies climate variability operating grant and while WHL was supported under a National Science Foundation Graduate Fellowship and a NASA Global Change Fellowship.

References

Assur, A., Composition of sea ice and its tensile strength, in *Arctic Sea Ice*, *N. A. S. N. R. C. Publ.*, 598, 106-138, 1958.

Bettge, T. W., J. W. Weatherly, W. M. Washington, D. Pollard, B. P. Briegleb, and W. G. Strand Jr., The NCAR CSM sea ice model, *NCAR Tech. Note, TN-425+STR*, 25 pp., Natl. Cent. for Atmos. Res., Boulder, Colo., 1996.

Bitz, C. M., D. S. Battisti, R. E. Moritz, and J. A. Beesley, Low frequency variability in the arctic atmosphere, sea ice, and upper ocean system, *J. Clim.*, *9*, 394–408, 1996.

Björk, G., On the response of the equilibrium thickness distribution of sea ice to ice export, mechanical deformation and thermal forcing with application to the Arctic Ocean, *J. Geophys. Res.*, *97*, 11,287–11,298, 1992.

Cox, G. F. N., and W. S. Weeks, Salinity variations in sea ice, *J. Glaciol.*, *13*, 109–120, 1974.

Ebert, E. E., and J. A. Curry, An intermediate one-dimensional thermodynamic sea ice model for investigating ice-atmosphere interactions, *J. Geophys. Res.*, *98*, 10,085–10,109, 1993.

Eicken, H., Salinity profiles of Antarctic sea ice: Field data and model results, *J. Geophys. Res.*, *97*, 15,545–15,557, 1992.

Eicken, H., M. Lensu, M. Leppäranta, W. B. Tucker III, A. J. Gow, and O. Salmela, Thickness, structure, and properties of level summer multiyear ice in the Eurasian sector of the Arctic Ocean, *J. Geophys. Res.*, *100*, 22,697–22,710, 1995.

Flato, G. M., and R. D. Brown, Variability and climate sensitivity of landfast Arctic sea ice, *J. Geophys. Res.*, *101*, 25,767–25,777, 1996.

Fletcher, J. O., The heat budget of the Arctic Basin and its relation to world climate, *Tech. Rep. R-444-PR*, 179 pp., The Rand Corp., Santa Monica, Calif., 1965.

Gabison, R., A thermodynamic model of the formation, growth, and decay of first-year sea ice, *J. Glaciol.*, *33*, 105–119, 1987.

Grenfell, T. C., and G. A. Maykut, The optical properties of ice and snow in the Arctic Basin, *J. Glaciol.*, *18*, 445–463, 1977.

Lipscomb, W. H., Modeling the thickness distribution of Arctic sea ice, Ph.D. thesis, 155 pp., Dep. of Atmos. Sci., Univ. of Wash., Seattle, 1998.

Malmgren, F., On the properties of sea ice, in *The Norwegian North Polar Expedition with the 'Maud' 1918-1925*, edited by H. U. Svedrup, vol. 1a no. 5, pp. 1–67, printed by John Griegs Boktr., Bergen, Norway, 1927.

Maykut, G. A., and N. Untersteiner, Some results from a time-dependent thermodynamic model of sea ice, *J. Geophys. Res.*, *76*, 1550–1575, 1971.

Maykut, G. A., T. C. Grenfell, and W. F. Weeks, On estimating spatial and temporal variations in the properties of ice in the polar oceans, *J. Mar. Syst.*, *3*, 41–72, 1992.

Ono, N., Specific heat and heat of fusion of sea ice, in *Physics of Snow and Ice*, edited by H. Oura, vol. 1, pp. 599–610, Inst. of Low Temp. Sci., Hokkaido, Japan, 1967.

Schwarzacher, W., Pack ice studies in the Arctic Ocean, *J. Geophys. Res.*, *64*, 2357–2367, 1959.

Schwerdtfeger, P., The thermal properties of sea ice, *J. Glac.*, *4*, 789–807, 1963.

Semtner, A. J., A model for the thermodynamic growth of sea ice in numerical investigations of climate, *J. Phys. Oceanogr.*, *6*, 379–389, 1976.

Semtner, A. J., On modelling the seasonal thermodynamic cycle of sea ice in studies of climatic change, *Clim. Change*, *6*, 27–37, 1984.

Tucker, W. B., III, A. J. Gow, and W. F. Weeks, Physical properties of summer sea ice in the Fram Strait, *J. Geophys. Res.*, *92*, 6787–6803, 1987.

Untersteiner, N., On the mass and heat budget of Arctic sea ice, *Arch. Meteorol. Geophys. Bioklimatol. Ser. A*, *12*, 151–182, 1961.

Untersteiner, N., Calculations of temperature regime and heat budget of sea ice in the Central Arctic, *J. Geophys. Res.*, *69*, 4755–4766, 1964.

Untersteiner, N., Natural desalination and equilibrium salinity profile of perennial sea ice, *J. Geophys. Res.*, *73*, 1251–1257, 1968.

Weeks, W. S., and S. F. Ackley, The growth, structure, and properties of sea ice, in *The Geophysics of Sea Ice, NATO ASI Ser., Ser. B*, vol. 146, edited by N. Untersteiner, pp. 9–164, Plenum, New York, 1986.

C. M. Bitz, Quaternary Research Center, MS 351360, University of Washington, Seattle, WA 98195-1360. (bitz@atmos.washington.edu)

William H. Lipscomb, Group T-3, MS B296, Los Alamos National Laboratory, Los Alamos, NM 87545.

(Received April 3, 1998; revised March 6, 1999; accepted March 19, 1999.)